

Thermal stability of thin-film periodic IZO structures with gradient modulation of oxygen content across the thickness

© A.K. Akhmedov¹, A.Sh. Asvarov¹, E.K. Murliev¹, A.Kh. Abduev²

¹ Amirkhanov Institute of Physics, Daghestan Federal Research Center, Russian Academy of Sciences, Makhachkala, Russia

² Federal State University of Education, Moscow, Russia

E-mail: cht-if-ran@mail.ru

Received August 10, 2024

Revised November 13, 2024

Accepted November 13, 2024

By periodically varying the oxygen content in working gas during high-frequency magnetron sputtering of the target consisting of In_2O_3 with 10 wt.% ZnO (IZO), high conductivity thin-film transparent periodic structures with the gradient-modulated oxygen content across the thickness were fabricated. Thermal stability of electrical properties of the obtained structures was investigated through annealing them both in vacuum and in open air. It was found out that the structure resistance increases in both annealing scenarios. The study has demonstrated that during annealing in air the resistance increase is caused primarily by reduction in the free electron concentration. This reduction is attributed to neutralization of vacancy donor centers by atmospheric oxygen. In contrast, the resistance increase during vacuum annealing is caused mainly by a decrease in the electron mobility resulting from degradation of the modulated (gradient) structure of the film.

Keywords: magnetron sputtering, indium oxide, zinc oxide, thin-film periodic structure, gradient modulation, electrical resistance.

DOI: 10.61011/TPL.2025.03.60725.20085

Transparent conductive layers based on doped wide-bandgap oxides (e.g. $\text{In}_2\text{O}_3:\text{Sn}$ (ITO), $\text{SnO}_2:\text{F}$, $\text{ZnO}:\text{Ga}$, etc.) characterized by high electrical conductivity and high optical transmittance in the visible spectrum range have become widely used in fabricating transparent electrodes in various optoelectronic applications [1–3]. Those materials (transparent conducting oxides, TCO) are characterized by a remarkable phenomenology. Even being undoped, TCO layers are characterized by a relatively high n -type intrinsic conductivity caused by high concentration of free charge carriers (10^{17} – 10^{19} cm^{-3}) resulting from deviation of their stoichiometry towards oxygen deficiency [4]. In turn, doping of these oxides with a donor impurity leads to an increase in the free charge carrier concentration up to $2 \cdot 10^{21}$ cm^{-3} [1–3]. Thus, unlike most other transparent dielectrics, TCO materials do not exhibit the phenomenon of electroactive impurity self-compensation by intrinsic acceptor-type defects [5]. At present, the lowest specific resistances have been achieved in transparent ITO electrodes: $\rho = (0.9\text{--}2) \cdot 10^{-4}$ $\Omega \cdot \text{cm}$ [2,3]. However, obtaining low-resistance transparent conductive ITO layers implies a high-temperature synthesis mode, since they, similarly to TCO based on ZnO and SnO_2 , possess the so-called „threshold temperature“ necessary for activating the dopant (e.g. $T \geq 200$ °C for Sn in ITO). At the same time, new requirements imposed on components of the rapidly developing industry of flexible transparent electronics on polymer carriers have intensified various-direction searching for new promising materials and low-temperature technological solutions for producing transparent electrodes [6,7]. One of those directions is the transition

from single TCO layers to multilayer oxide/metal/oxide structures [8,9]. Another promising direction seems to be using as transparent electrodes low-temperature layers based on amorphous ionic oxide systems, e.g. $a\text{-In}_2\text{O}_3$, doped with Zn (IZO) [10,11]. In such a system, the dopant does not play the role of a classical donor impurity but stabilizes in In_2O_3 an amorphous state with a high intrinsic donor concentration (V_{O}) and high charge carrier Hall mobility caused by direct overlap of the s - orbitals of neighboring cations [12].

Earlier in [13] we have shown by the example of the IZO system that, in the case of low-temperature deposition (substrate temperature $T = 100$ °C) in the inert Ar environment, IZO layers are characterized by high charge carrier concentration $n = 6.8 \cdot 10^{20}$ cm^{-3} with mobility $\mu = 26.4$ $\text{cm}^2 \cdot \text{V}^{-1} \cdot \text{s}^{-1}$ and specific resistance $\rho = 3.5 \cdot 10^{-4}$ $\Omega \cdot \text{cm}$ (hereinafter these layers are designated as $n\text{-IZO}$). In turn, being sputtered in the $\text{Ar}/\text{O}_2 = 99.6/0.4$ environment, IZO layers are distinguished by increased Hall mobility $\mu = 37.9$ $\text{cm}^2 \cdot \text{V}^{-1} \cdot \text{s}^{-1}$ at $n = 3.0 \cdot 10^{20}$ cm^{-3} and $\rho = 5.6 \cdot 10^{-4}$ $\Omega \cdot \text{cm}$ (hereinafter these layers are designated as $\mu\text{-IZO}$). Note here that specific resistances of the IZO layers were in both cases lower than those characteristic of ITO layers deposited at low temperatures [1–3].

After that, using the observed dependence of thin-film IZO electrical characteristics on the O_2 content in working gas, we have tested a concept for improving electrical characteristics of TCO materials; the concept was theoretically considered for the first time in [14]. According to this concept, carrier transport in TCO materials may be

Electrical characteristics of the modulated IZO_{mod} structure before and after annealing

Sample type	$T_{ann},$ $^{\circ}\text{C}$	$\rho,$ $10^{-4} \Omega \cdot \text{cm}$	$n,$ 10^{20} cm^{-3}	$\mu,$ $\text{cm}^2 \cdot \text{V}^{-1} \cdot \text{s}^{-1}$
Initial IZO_{mod} sample	–	2.9	5.8	37.0
Sample IZO_{mod} after vacuum annealing	150	3.1	5.8	35.3
	250	3.5	6.5	27.6
Sample IZO_{mod} after annealing in air	150	3.2	5.3	37.5
	250	18.6	0.8	42.8

improved by replacing a single TCO layer with a multilayer periodic structure consisting of alternating oxide layers with high free electron concentration and layers with high electron mobility. In such a structure, reduction of charge carriers scattering at ionized donor centers is assumed to be caused by their spatial separation from the main electron transport paths. In the context of testing this concept based on a single ionic oxide system IZO, we obtained transparent conducting thin-film IZO_{mod} structures consisting of multiple repeating layer pairs n -IZO/ μ -IZO [15]. The layer thicknesses and number of their pairs were controlled by means of programmable modulation of the oxygen content in working gas during deposition. It was shown that the modulated IZO_{mod} structure with the optimized thickness ($d = 336 \text{ nm}$) and architecture consisting of alternating n -IZO layers 4 nm thick and μ -IZO layers 2 nm thick exhibits resistivity $\rho = 2.9 \cdot 10^{-4} \Omega \cdot \text{cm}$ that is record-low for low-temperature TCO materials. This stems from the fact that in this structure free electron's Hall mobility $\mu = 37.0 \text{ cm}^2 \cdot \text{V}^{-1} \cdot \text{s}^{-1}$ that is close to that in the μ -IZO layer is combined with a relatively high free carrier concentration $n = 5.8 \cdot 10^{20} \text{ cm}^{-3}$ comparable to the concentration achieved in the continuous n -IZO layer.

It is known that, in addition to high electrical and optical quality, there is another important requirement for transparent conductive layers, namely, temperature stability of their functional properties [16]. Here we have studied stability of the oxygen modulated state in synthesized periodic IZO_{mod} structure to the vacuum and open-air annealing. One of the synthesized IZO_{mod} samples was subjected to successive hour-long annealings at the temperature (T_{ann}) of 150 and 250 $^{\circ}\text{C}$ in vacuum ($P = 2 \cdot 10^{-4} \text{ Pa}$). Along with this, another IZO_{mod} sample was annealed under identical temperature conditions in open air. The rate of temperature growth to T_{ann} was 20 $^{\circ}\text{C}/\text{min}$ in both cases.

According to the data of transmission electron microscopy (TEM) (Tecnai Osiris FEI, USA), the initial IZO_{mod} sample had a dense uniform amorphous structure free of visible structuring elements and smooth surface morphology (Fig. 1). Results of electron diffraction studies of the annealed samples, as well as data from their XRD analysis with diffractometer X'PERT PRO PANalytical, Netherlands,

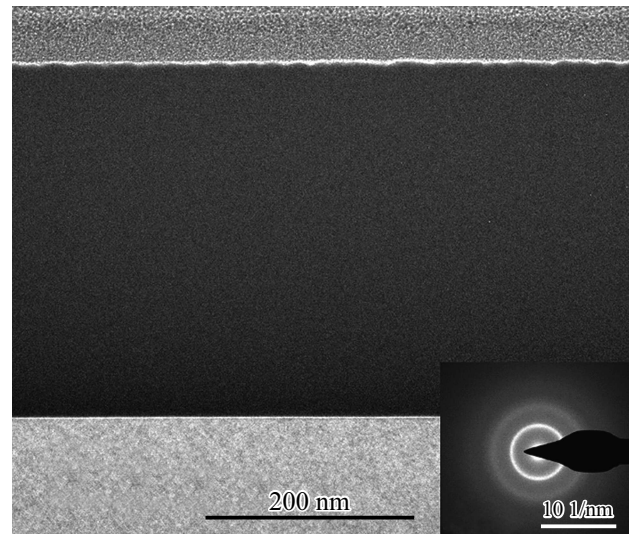


Figure 1. TEM micrograph of the initial IZO_{mod} sample. The inset presents the electron diffraction pattern of the IZO_{mod} structure middle section.

indicated that, regardless of the annealing type, the amorphous state of thin-film periodic IZO_{mod} structures remains unchanged in the considered temperature range.

The effect of vacuum and air annealing on electrical characteristics of the thin-film periodic IZO_{mod} structure is demonstrated in the Table.

One can see that, if vacuum annealing at $T_{ann} = 150^{\circ}\text{C}$ is accompanied by a slight increase in specific resistance (by $< 7\%$), then subsequent annealing at 250 $^{\circ}\text{C}$ leads to a more significant (by 20%) increase to $\rho = 3.5 \cdot 10^{-4} \Omega \cdot \text{cm}$ that is characteristic of a uniform single n -IZO layer. Note that the increase in specific resistance during vacuum annealing occurs due to a decrease in the charge-carrier Hall mobility. We assume that the observed increase in resistance is caused by a decrease in the depth of oxygen modulation across the structure thickness due to the interlayer oxygen diffusion. A slight increase in the free electron concentration may be caused by thermal oxygen desorption from the structure surface and associated increase in the number of surface donor-vacancy centers.

In the case of open-air annealing, one can see that the IZO_{mod} structure specific resistance increases because of a decrease in the free electron concentration. When $T_{ann} = 150^{\circ}\text{C}$, relative variation in resistance is insignificant (about 10%). However, when the annealing temperature increases to 250 $^{\circ}\text{C}$, the sample specific resistance increases by more than 6 times due to an increase in the rate of the atmospheric oxygen diffusion from the structure surface into its bulk. Therewith, the increase in resistance is accompanied by an increase in Hall mobility, which results from reduction of charge carrier scattering with decreasing concentration of V_O defects in IZO.

These data are in good agreement with the results of pre-annealing and post-annealing studies of IZO_{mod} by op-

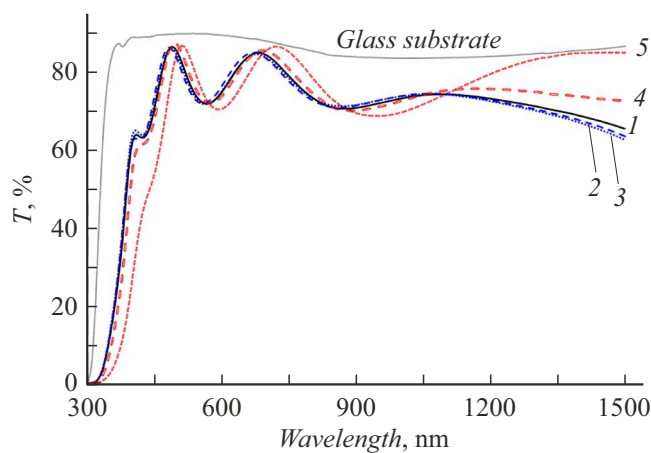


Figure 2. Optical transmission spectra of the modulated thin-film IZO_{mod} structure before and after annealing. 1 — initial sample, 2 — sample after vacuum annealing at 150°C , 3 — sample after vacuum annealing at 250°C , 4 — sample after annealing in air at 150°C , 5 — sample after annealing in air at 250°C .

tical spectrometry (spectrophotometer UV-3600 Shimadzu, Japan). Optical transmission spectra presented in Fig. 2 show that, near the fundamental absorption edge (FAE), all the spectra, except for that of the structure annealed in air at 250°C , are almost fully coincident. This evidences that vacuum annealings and annealing in open air at 150°C do not induce significant variations in the free electron concentration. In the spectrum of the structure annealed in open air at 250°C there was observed a FAE shift to the long-wavelength region which, together with the observed enhancement of the near-infrared transmission, indicates a sharp decrease in the free electron concentration.

Fig. 3 presents the distribution profiles of elements In, O and Zn across the thickness for the initial IZO_{mod} sample and also for the samples that have undergone successive stages of annealing in vacuum and air. The profiles were obtained from the data of EDX spectroscopy performed along with TEM examination of the IZO_{mod} microstructure. All the three profiles exhibit highly uniform zinc distributions. In the initial structure, the indium and oxygen distribution curves exhibit small (about 2–3 at.%) fluctuations and more significant (up to 10 at.%) nonuniformity across the structure thickness. The observed minor fluctuations in the indium and oxygen distributions are apparently associated with the oxygen content modulation initially introduced in the sample. The O/In ratio is minimal in the middle of the sample and gradually increases when approaching the sample edges. Vacuum annealing made the oxygen and indium profiles smoother and straighter. We suppose that the profiles became smoother mainly due to the oxygen interlayer diffusion, while the oxygen profile alignment occurred due to the oxygen thermal desorption from the surface. In the case of atmospheric annealing, the oxygen content increases; the especially rapid increase takes place near the surface (up to 70 nm), which evidences that

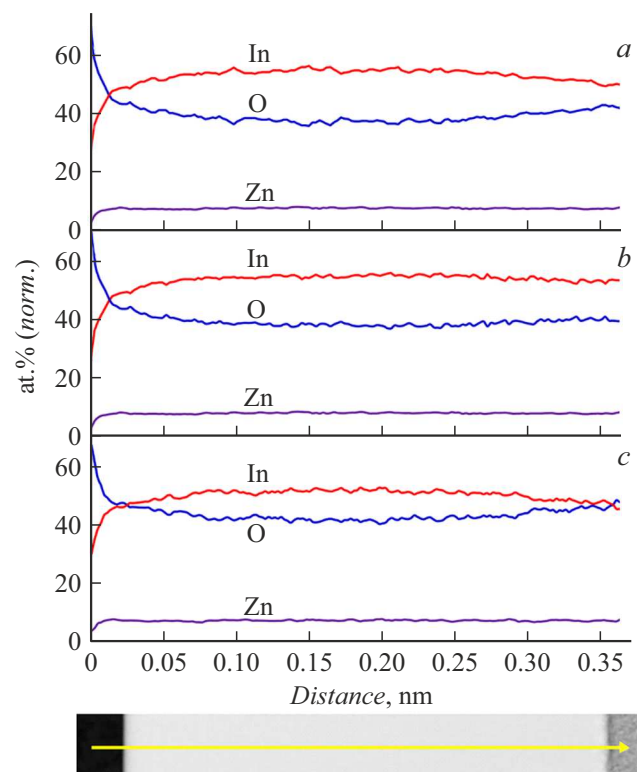


Figure 3. The In, Zn and O distribution profiles across the thickness in the IZO_{mod} structure. a — initial sample, b — sample after vacuum annealings, c — sample after annealings in air.

atmospheric oxygen diffuses from the structure surface to the bulk.

The studies performed have shown high stability of the oxygen modulated state in the synthesized periodic structure to the vacuum and open-air annealing at $T_{ann} \leq 150^\circ\text{C}$. To our mind, high density and amorphous structure of the IZO_{mod} samples make impossible the mechanisms of rapid atmospheric oxygen diffusion through pores and grain boundaries, and the observed interlayer and transverse oxygen diffusion proceeds predominantly via the slower vacancy mechanism.

Funding

The study was performed with the support from the Russian Science Foundation (project № 22-19-00157) and by using the equipment of Analytical shared equipment center of Daghestan Federal Research Center of RAS and shared equipment center „Structural Diagnostics of Materials“ of NRC „Kurchatov Institute“.

Conflict of interests

The authors declare that they have no conflict of interests.

References

- [1] Y. Zhidik, A. Ivanova, S. Smirnov, K. Zhuk, I. Yunusov, P. Troyan, *Coatings*, **12** (12), 1868 (2022).
DOI: 10.3390/coatings12121868
- [2] H. Liu, V. Avrutin, N. Izyumskaya, Ü. Özgür, H. Morkoç, *Superlat. Microstruct.*, **48**, 458 (2010).
DOI: 10.1016/j.spmi.2010.08.011
- [3] Y.S. Zhidik, P.E. Troyan, V.V. Kozik, S.A. Kozyukhin, A.V. Zabolotskaya, S.A. Kuznetsova, *Russ. Phys. J.*, **63** (7), 1139 (2020). DOI: 10.1007/s11182-020-02167-4.
- [4] D.C. Look, J.W. Hemsky, J.R. Sizelove, *Phys. Rev. Lett.*, **82**, 2552 (1999). DOI: 10.1103/PhysRevLett.82.2552
- [5] A. Zunger, *Appl. Phys. Lett.*, **83**, 57 (2003).
DOI: 10.1063/1.1584074
- [6] R.J. Hamers, *Nature*, **412**, 489 (2001).
DOI: 10.1038/35087682
- [7] Y. Liu, M. Pharr, G.A. Salvatore, *ACS Nano*, **11**, 9614 (2017).
DOI: 10.1021/acsnano.7b04898
- [8] P. Zhao, S. Kim, S. Yoon, P. Song, *Thin Solid Films*, **665**, 137 (2018). DOI: 10.1016/j.tsf.2018.09.018
- [9] A.K. Akhmedov, A.Kh. Abduev, V.M. Kanevsky, A.E. Muslimov, A.Sh. Asvarov, *Coating*, **10** (3), 269 (2020).
DOI: 10.3390/coatings10030269
- [10] H. Hara, T. Hanada, T. Shiro, T. Yatabe, *J. Vac. Sci. Technol. A*, **22** (4), 1726 (2004). DOI: 10.1116/1.1692270
- [11] S. Li, Z. Shi, Z. Tang, X. Li, *Vacuum*, **145**, 262 (2017).
DOI: 10.1016/j.vacuum.2017.09.011
- [12] H. Hosono, *J. Non-Cryst. Solids*, **352**, 851 (2006).
DOI: 10.1016/j.jnoncrysol.2006.01.073
- [13] A.K. Akhmedov, E.K. Murliev, A.Sh. Asvarov, A.E. Muslimov, V.M. Kanevsky, *Coating*, **12** (10), 1583 (2022).
DOI: 10.3390/coatings12101583
- [14] J.J. Robbins, C.A. Wolden, *Appl. Phys. Lett.*, **83** (19), 3933 (2003). DOI: 10.1063/1.1625435
- [15] A.K. Akhmedov, A.K. Abduev, E.K. Murliev, V.V. Belyaev, A.S. Asvarov, *Materials*, **16**, 3740 (2023).
DOI: 10.3390/ma16103740
- [16] A.Sh. Asvarov, A.K. Akhmedov, A.E. Muslimov, V.M. Kanevsky, *Tech. Phys. Lett.*, **48** (1), 91 (2022).
DOI: 10.21883/TPL.2022.01.52481.19001.

Translated by EgoTranslating